

THE REDSHIFT AND NATURE OF AZTEC/COSMOS 1: A STARBURST GALAXY AT  $Z = 4.6$ 

V. SMOLČIĆ<sup>1,2</sup>, P. ČAPAK<sup>3,4</sup>, O. ILBERT<sup>5</sup>, A.W. BLAIN<sup>3</sup>, M. SALVATO<sup>3,9</sup>, I. ARETXAGA<sup>14</sup>, E. SCHINNERER<sup>23</sup>, D. MASTERS<sup>3,6</sup>, I. MORIĆ<sup>3,7</sup>, D. A. RIECHERS<sup>3,8</sup>, K. SHETH<sup>4</sup>, M. ARAVENA<sup>10</sup>, H. AUSSEL<sup>11</sup>, J. AGUIRRE<sup>12,13</sup>, S. BERTA<sup>15</sup>, C. L. CARILLI<sup>16</sup>, F. CIVANO<sup>17</sup>, G. FAZIO<sup>17</sup>, J. HUANG<sup>17</sup>, D. HUGHES<sup>14</sup>, J. KARTALTEPE<sup>18</sup>, A. M. KOEKEMOER<sup>19</sup>, J.-P. KNEIB<sup>5</sup>, E. LEFLOC'H<sup>18,20</sup>, D. LUTZ<sup>15</sup>, H. MCCRACKEN<sup>5</sup>, B. MOBASHER<sup>6</sup>, E. MURPHY<sup>4</sup>, F. POZZI<sup>21</sup>, L. RIGUCCINI<sup>22</sup>, D. B. SANDERS<sup>18</sup>, M. SARGENT<sup>23</sup>, K. S. SCOTT<sup>24</sup>, N.Z. SCOVILLE<sup>3</sup>, Y. TANIGUCHI<sup>25</sup>, D. THOMPSON<sup>26</sup>, C. WILLOTT<sup>27</sup>, G. WILSON<sup>28</sup>, M. YUN<sup>28</sup>

## ABSTRACT

Based on broad/narrow-band photometry and Keck DEIMOS spectroscopy we report a redshift of  $z = 4.64_{-0.08}^{+0.06}$  for AzTEC/COSMOS 1, the brightest sub-mm galaxy in the AzTEC/COSMOS field. In addition to the COSMOS-survey X-ray to radio data, we report observations of the source with Herschel/PACS (100, 160  $\mu\text{m}$ ), CSO/SHARC II (350  $\mu\text{m}$ ), CARMA and PdBI (3 mm). We do not detect CO(5  $\rightarrow$  4) line emission in the covered redshift ranges, 4.56-4.76 (PdBI/CARMA) and 4.94-5.02 (CARMA). If the line is within this bandwidth, this sets  $3\sigma$  upper limits on the gas mass to  $\lesssim 8 \times 10^9 M_{\odot}$  and  $\lesssim 5 \times 10^{10} M_{\odot}$ , respectively (assuming similar conditions as observed in  $z \sim 2$  SMGs). This could be explained by a low CO-excitation in the source. Our analysis of the UV-IR spectral energy distribution of AzTEC 1 shows that it is an extremely young ( $\lesssim 50$  Myr), massive ( $M_{*} \sim 10^{11} M_{\odot}$ ), but compact ( $\lesssim 2$  kpc) galaxy forming stars at a rate of  $\sim 1300 M_{\odot} \text{yr}^{-1}$ . Our results imply that AzTEC 1 is forming stars in a 'gravitationally bound' regime in which gravity prohibits the formation of a superwind, leading to matter accumulation within the galaxy and further generations of star formation.

*Subject headings:* galaxies: distances and redshifts – galaxies: high-redshift – galaxies: active – galaxies: starburst – galaxies: fundamental parameters

<sup>1</sup> ESO ALMA COFUND Fellow, European Southern Observatory, Karl-Schwarzschild-Strasse 2, 85748 Garching b. Muenchen, Germany

<sup>2</sup> Argelander Institut for Astronomy, Auf dem Hügel 71, Bonn, 53121, Germany

<sup>3</sup> California Institute of Technology, MC 249-17, 1200 East California Boulevard, Pasadena, CA 91125

<sup>4</sup> Spitzer Science Center, 314-6 Caltech, 1201 E. California Blvd. Pasadena, CA, 91125

<sup>5</sup> Laboratoire d'Astrophysique de Marseille, Université de Provence, CNRS, BP 8, Traverse du Siphon, 13376 Marseille Cedex 12, France

<sup>6</sup> Department of Physics and Astronomy, University of California, Riverside, CA, 92521, USA

<sup>7</sup> University of Zagreb, Physics Department, Bijenička cesta 32, 10000 Zagreb, Croatia

<sup>8</sup> Hubble Fellow

<sup>9</sup> Max-Planck-Institut für Plasmaphysik, Boltzmanstrasse 2, Garching 85748, Germany

<sup>10</sup> National Radio Astronomy Observatory, 520 Edgemont Road, Charlottesville, VA 22903, USA

<sup>11</sup> UMR AIM (CEA-UP7-CNRS), CEA-Saclay, Orme des Merisiers, bt. 709, F-91191 Gif-sur-Yvette Cedex, France

<sup>12</sup> Jansky Fellow, National Radio Astronomy Observatory  
<sup>13</sup> University of Pennsylvania, Department of Physics and Astronomy, 209 South 33rd Street, Philadelphia, PA 19104

<sup>14</sup> Instituto Nacional de Astrofísica, Óptica y Electrónica (INAOE), Aptdo. Postal 51 y 216, 72000 Puebla, Pue., Mexico

<sup>15</sup> Max-Planck-Institut für extraterrestrische Physik, Postfach 1312, 85741 Garching, Germany

<sup>16</sup> National Radio Astronomy Observatory, P.O. Box 0, Socorro, NM 87801-0387

<sup>17</sup> Harvard-Smithsonian Centre for Astrophysics, 60 Garden Street, Cambridge, MA 02138, USA

<sup>18</sup> Institute for Astronomy, University of Hawaii, 2680 Woodlawn Drive, Honolulu, HI, 96822, USA

<sup>19</sup> Space Telescope Science Institute, 3700 San Martin Drive, Baltimore, MD 21218

<sup>20</sup> Spitzer Fellow

<sup>21</sup> INAF Osservatorio Astronomico di Roma, via di Frascati

33, 00040 Monte Porzio Catone, Italy

<sup>22</sup> Laboratoire AIM-Paris-Saclay, CEA/DSM/Irfu CNRS Université Paris Diderot, CE-Saclay, pt courrier 131, F-91191 Gif-sur-Yvette, France

<sup>23</sup> Max Planck Institut für Astronomie, Königstuhl 17, Heidelberg, D-69117, Germany

<sup>24</sup> Department of Physics and Astronomy, University of Pennsylvania, Philadelphia PA, 19104

<sup>25</sup> Research Center for Space and Cosmic Evolution, Ehime University, Bunkyo-cho 2-5, Matsuyama 790-8577, Japan

<sup>26</sup> Large Binocular Telescope Observatory, University of Arizona, 933 N. Cherry Ave., Tucson, AZ, 85721, USA

<sup>27</sup> Herzberg Institute of Astrophysics, National Research Council, 5071 West Saanich Rd., Victoria, BC V9E 2E7, Canada

<sup>28</sup> Department of Astronomy, University of Massachusetts, Amherst, MA 01003, USA

\* Based on observations with: the W.M. Keck Observatory, the Canada-France-Hawaii Telescope; the United Kingdom Infrared Telescope; the Subaru Telescope; the NASA/ESA *Hubble Space Telescope*; the NASA Spitzer Telescope; the Caltech Submillimeter Observatory; the Smithsonian Millimeter Array; and the National Radio Astronomy Observatory. Herschel is an ESA space observatory with science instruments provided by European-led Principal Investigator consortia and with important participation from NASA.

## 1. INTRODUCTION

Submillimeter galaxies (SMGs;  $S_{850\mu\text{m}} > 5$  mJy) are ultra-luminous, dusty starbursting systems with extreme star formation rates ( $\text{SFR} \sim 100 - 1000 M_{\odot} \text{yr}^{-1}$ ; e.g. Blain et al. 2002). The bulk of this population has been shown to lie at  $2 < z < 3$  (e.g. Chapman et al. 2005). However, only recently have blank-field sub-mm surveys started to discover the high-redshift ( $z > 4$ ) tail of the SMG distribution. To date seven  $z > 4$  SMGs have been spectroscopically confirmed (and published: three in GOODS-N, Daddi et al. 2009a,b; two in COSMOS, Capak et al. 2008; Schinnerer et al. 2008; Riechers et al. 2010; Capak et al. 2010, one in ECDFS, Coppin et al. 2009, 2010; and one in Abell 2218, Knudsen et al. 2010). These high-redshift SMGs, presenting a challenge to cosmological models of structure growth (see e.g. Coppin et al. 2009), may alter our understanding of the role of SMGs in galaxy evolution.

Galaxies are thought to evolve in time from an initial stage with irregular/spiral morphology towards passive, very massive elliptical systems ( $M_* > 10^{11} M_{\odot}$ ; Faber et al. e.g. 2007). The morphology and spectral properties of passive galaxies indicate that they have formed in a single intense burst at  $z > 4$  (e.g. Cimatti et al. 2008). SMGs represent short-lasting ( $\ll 100$  Myr) starburst episodes of the highest known intensity. Thus, they would be the perfect candidates for  $z \sim 2$  passive galaxy progenitors. In this Letter we report on a new  $z > 4$  SMG – AzTEC/COSMOS 1 (AzTEC 1 hereafter), the brightest SMG detected in the AzTEC-COSMOS field (Scott et al. 2008).

We adopt  $H_0 = 70$ ,  $\Omega_M = 0.3$ ,  $\Omega_{\Lambda} = 0.7$ , use a Salpeter initial mass function, and AB magnitudes.

## 2. DATA

The available photometric (X-ray–radio) data for AzTEC 1 ( $\alpha = 09 : 59 : 42.863$ ,  $\delta = +02 : 29 : 38.19$ ) are summarized in `tab:phot`. Its optical/IR counterpart – identified by Younger et al. (2007) in follow-up SMA observations of the original JCMT/AzTEC 1.1 mm detection (Scott et al. 2008) – has been targeted by the COSMOS project (Scoville et al. 2007) in more than 30 filters: ground-based optical/NIR imaging in 22 bands (Capak et al. 2007)<sup>30</sup>, Chandra (Elvis et al. 2009), GALEX (Zamojski et al. 2007), HST (Scoville et al. 2007; Koekemoer et al. 2009; Leauthaud et al. 2007), Spitzer (Sanders et al. 2007), and VLA (Schinnerer et al. 2007, 2010, Smolčić et al., in prep.) (see `tab:phot`).

Herschel (100 and 160  $\mu\text{m}$ ) data are drawn from the PACS Evolutionary Probe observations (Lutz et al., in prep; Berta et al. 2010).

Observations at 350  $\mu\text{m}$  with CSO/SHARC II were obtained during two nights in March/2009 with an average 225 GHz opacity of  $\tau_{225} < 0.05$ . The data were reduced using the standard CRUSH tool. A total of  $\sim 6$  hrs of integration time reached an rms of 10 mJy. Combined with previous data (Aguirre et al., in prep) we detect no flux at  $1\sigma = 7$  mJy.

Observations at 3 mm were obtained with CARMA in

E-array configuration in July/2009. The target was observed for 8.5 hrs on-source. The 3 mm receivers were tuned to 98.95 GHz (3.03 mm), with lower (upper) sidebands centered at 96.43 (101.46) GHz, respectively. Each sideband was observed with 45 31.25 MHz wide channels, leading to a total bandwidth of 2.56 GHz. The data reduction was performed with the MIRIAD package. No line emission (the CO(5 $\rightarrow$ 4) transition is expected at the source’s redshift) was detected across the observed bands covering  $4.64 < z < 4.72$  and  $4.94 < z < 5.02$ . The uv-data were imaged merging both sidebands together and using natural weighting. We infer an rms of 0.36 mJy/beam in the continuum map, but no detection of the source.

Using the new WideX correlator on PdBI, AzTEC-1 was observed with 6 antennas in Apr/May/2010 for  $\sim 5.5$  hrs on-source. The WideX correlator covered 3.6 GHz bandwidth using polarizations centered at 101.866394 GHz. 1005+066 and 3C273 were used as phase and gain calibrators, respectively. The flux calibration error is estimated to be  $< 10\%$ . The naturally weighted beam is  $6.38'' \times 5.01''$  (PA  $32^\circ$ ). The 3 mm continuum emission, shown in Fig. 1, is detected at  $7.5\sigma$  with  $S_{3\text{mm}} = 0.3 \pm 0.04$  mJy and unresolved. No line emission is detected across the band covering  $4.56 < z < 4.76$ . The rms per 180 km/s wide channel (61.2 MHz) is 0.35 mJy/beam.

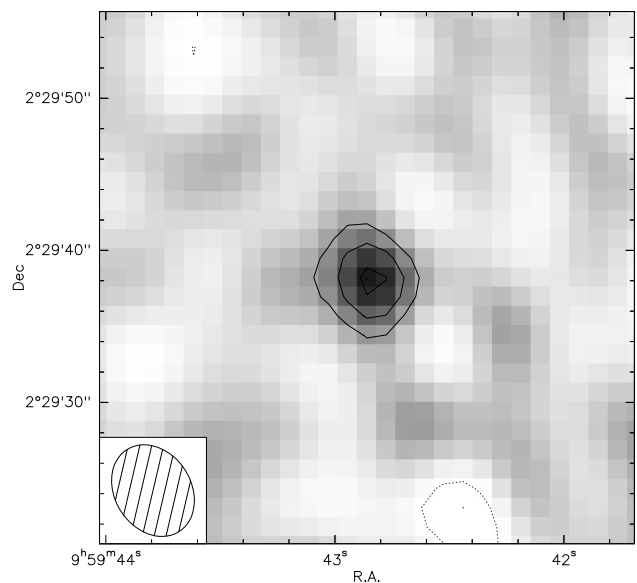


FIG. 1.— PdBI 3 mm continuum image of AzTEC 1. Contours are at  $\pm 3\sigma$ ,  $\pm 5\sigma$ ,  $\pm 7\sigma$  ( $1\sigma = 0.04$  mJy/beam). The inset shows the clean beam.

AzTEC 1 was spectroscopically targeted with DEIMOS on Keck-II in Nov/2008 with clear conditions and  $\sim 1''$  seeing and a 4 hr integration time split into 30 min exposures. The data were collected with the 830l/mm grating tilted to 7900  $\text{\AA}$  and the OG550 blocker. The objects were dithered  $\pm 3''$  along the slit to remove ghosting.

The data were reduced via the modified DEEP2 DEIMOS pipeline (see Capak et al. 2008). The over-

<sup>30</sup> An updated version of the UV-NIR catalog, available at <http://irsa.ipac.caltech.edu/data/COSMOS/tables/photometry>, has been used.

all instrumental throughput was determined using the standard stars HZ-44 and GD-71. Bright stars in the mask were used to determine the amount of atmospheric extinction, wavelength dependent slit losses from atmospheric dispersion, and to correct for the A, B, and water absorption bands. The 2D- and 1D- spectra are shown in Fig. 2. No strong emission lines are present in the spectrum. The continuum is clearly detected (see 2D-spectrum in Fig. 2), however at low signal-to-noise, consistent with the faint magnitude of the source ( $i^+ = 25.2$ ).

### 3. THE REDSHIFT OF AZTEC 1

From features in the DEIMOS spectrum we determine a redshift for AzTEC 1 of  $4.650 \pm 0.005$  based on the blue cut-off of Ly $\alpha$ . Note that in this redshift range, Ly $\alpha$ , the most prominent emission line that may be expected, would be attenuated by the atmospheric B-band (6860-6890 Å). The 1216 Å Ly $\alpha$  forest break is however clearly seen in the 2D-spectrum, as well as in the heavily smoothed 1D-spectrum (see Fig. 2, Fig. 3). If this were the 4000 Å break at  $z = 0.71$  we would expect strong 160  $\mu\text{m}$  and 350  $\mu\text{m}$  detections for any known galaxy type. As these do not exist for AzTEC 1, low redshifts ( $z < 1$ ) can be ruled out. Note that the inferred high redshift is consistent with both, the source being a B-band drop-out, and its FIR/radio ratio (Younger et al. 2008; Yum & Carilli 2002).

Due to a) the low S/N, b) the general absence of strong emission lines, and c) the atmospheric B-band bias at the expected position of Ly $\alpha$ , we utilize the photometric data available for AzTEC 1 along with the spectrum to refine our redshift estimate. Using 31 NUV-NIR photometric measurements (Tab. 1) and the binned spectrum we constrain the redshift via a  $\chi^2$  minimization SED fitting technique described in detail by Ilbert et al. (2009). Our best fit results, as well as the redshift probability [ $\exp(-\chi^2/2)$ ] distribution, are shown in Fig. 3. We find a redshift of  $z = 4.64^{+0.06}_{-0.08}$ , where the errors are drawn from the 68% confidence interval. Note that this analysis yields also a secondary redshift peak at  $z = 4.44$ , albeit with a significantly lower probability than that at  $z = 4.64$ .

As it is possible that heavy extinction in the UV biases UV-NIR-derived photometric redshifts towards higher values, we estimate the photometric redshift using FIR-radio data via a Monte-Carlo approach, described in detail in Aretxaga et al. (2003). We find that the upper limits at  $\lambda < 450 \mu\text{m}$  strongly suggest  $z > 4.0$  (at  $\sim 90\%$  confidence). The redshift probability distribution reaches a plateau with equally plausible solutions between  $z = 4.5$  and  $z = 6.0$ , supporting the optical-IR redshift solution.

The inferred most probable redshift  $z = 4.64$  (based on UV-NIR data) is close to the spectroscopically determined redshift of  $z = 4.65$ , and supported by the FIR-radio data. Thus, hereafter we take  $z = 4.64^{+0.06}_{-0.08}$  as the best estimate for the redshift of AzTEC 1.

### 4. SPECTRAL ENERGY DISTRIBUTION OF AZTEC 1

In Fig. 4 we show the SED of AzTEC 1. Fixing the redshift to  $z = 4.64$  (Sec. 3) we fit the UV-NIR SED using various model spectrum libraries. For each model

we compute the total  $\chi^2$  and define the most probable parameter values and their errors from the probability distribution function. Using the Bruzual et al. (2003) library (see Smolčić et al. 2008 for details) the UV-NIR SED is best described by a  $740^{+200}_{-60}$  Myr old starburst with  $\text{SFR} = 410 \pm 50 M_{\odot}/\text{yr}$ , an extinction of  $A_V = 2 \pm 0.2$  mag, and a stellar mass of  $M_* = (1.5 \pm 0.2) \times 10^{11} M_{\odot}$  (see top panel in Fig. 4). We find consistent results when using the Maraston (2005) library. However, as pointed out by Maraston et al. (2010), using exponentially decaying star formation histories as above some of the free parameters may be poorly parameterized in young starburst galaxies whose SED is dominated by the youngest stellar populations that outshine the old ones. Thus, we additionally fit to the optical-NIR SED of AzTEC 1 the model library presented in Efstathiou et al. (2000), specifically developed for starburst galaxies. These (UV-mm) models are treated as an ensemble of optically thick giant molecular clouds (GMCs) centrally illuminated by recently formed stars. The evolution of the stellar population within the GMC is modeled using the Bruzual et al. (2003) stellar population synthesis models. The Efstathiou et al. (2000) models yield a  $37 \pm 4$  Myr old starburst with  $A_V = 100 \pm 20$  and  $\text{SFR} = 1300 \pm 150 M_{\odot}/\text{yr}$ .

We fit the IR portion of the SED of AzTEC 1 (fixing  $z = 4.64$ ) using the Chary & Elbaz (2001; CE hereafter), Dale & Helou (2002), and Lagache et al. (2003) models. The best fit IR model, shown in Fig. 4 (bottom panel), is a Lagache et al. (2003) template with a total IR (8 – 1000  $\mu\text{m}$ ) luminosity of  $2.9 \times 10^{13} L_{\odot}$ , and a FIR (60 – 1000  $\mu\text{m}$ ) luminosity of  $9 \times 10^{12} L_{\odot}$ . For comparison, the CE SED models yield the second best fit with integrated luminosities a factor of 3-4 higher. Converting the (8 – 1000  $\mu\text{m}$ ) IR luminosity to a SFR, using the Kennicutt (1998) conversion, we find a SFR of  $\sim 1600 M_{\odot}/\text{yr}$ . To obtain the dust temperature and dust mass in AzTEC 1 we perform a gray-body dust model fit to the data as described in detail in Aravena et al. (2008). Using  $\beta = 1.5$  and  $\beta = 2$  we consistently find a dust temperature of  $T_D \sim 50$  K and dust mass of  $M_D \sim 1.5 \times 10^9 M_{\odot}$  (while the IR luminosity is within a factor of two compared to that given above).

## 5. DISCUSSION

### 5.1. Lack of molecular gas?

Based on observations of AzTEC 1 from radio to X-rays, and a Keck II/DEIMOS spectrum, we have shown that AzTEC 1 is a  $L_{\text{FIR}} = 9 \times 10^{12} L_{\odot}$  starburst galaxy at  $z = 4.64^{+0.06}_{-0.08}$  (the given errors are  $1\sigma$  uncertainties). However, contrary to expectations our searches for the CO(5 $\rightarrow$ 4) transition line ( $\nu_{\text{RF}} = 576.268$  GHz) in this galaxy with the PdBI/CARMA interferometers have yielded no detection. Assuming a line width of 500  $\text{km s}^{-1}$  the  $3\sigma$  limits in the line luminosity based on PdBI and CARMA observations are estimated to be  $L'_{\text{CO}} \lesssim 9.8 \times 10^9 \text{ K km s}^{-1} \text{ pc}^2$  ( $4.56 < z < 4.76$ ) and  $L'_{\text{CO}} \lesssim 6.5 \times 10^{10} \text{ K km s}^{-1} \text{ pc}^2$  ( $4.64 < z < 4.72$  and  $4.94 < z < 5.02$ ), respectively. Taking  $M_{\text{gas}}/L'_{\text{CO}} = 0.8 M_{\odot} (\text{K km s}^{-1} \text{ pc}^2)^{-1}$  (Downes & Solomon 1998) implies  $3\sigma$  gas mass upper limits of  $M_{\text{gas}} \lesssim 8 \times 10^9 M_{\odot}$  ( $4.56 < z < 4.76$ ) and  $M_{\text{gas}} \lesssim$

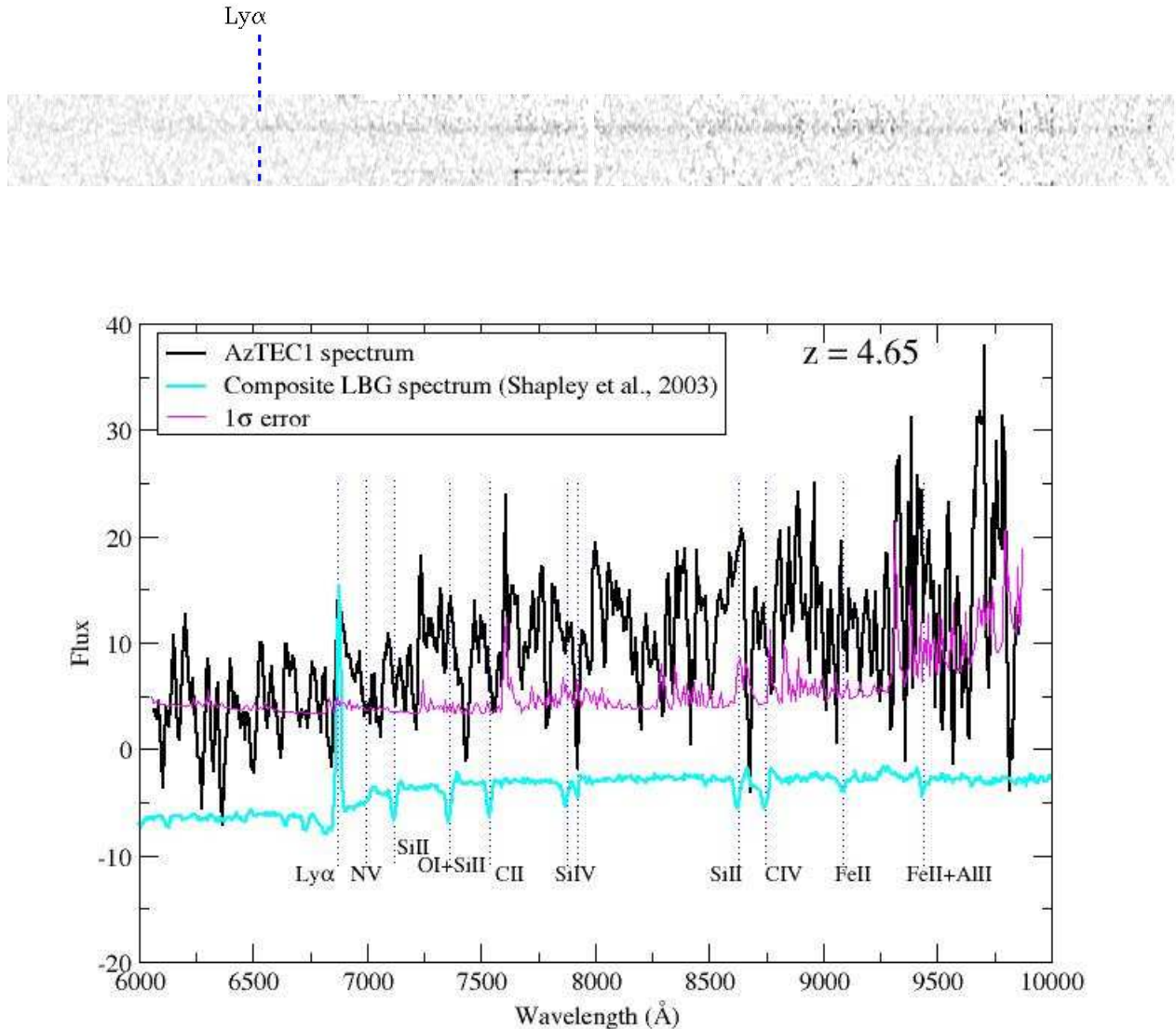


FIG. 2.— The top panel shows the Keck II/DEIMOS 2D-spectrum of AzTEC 1. Note the increase in continuum flux beyond Ly $\alpha$  (see also Fig. 3). In the bottom panel the extracted 1D-spectrum is shown. Note that the atmospheric B-band (6860–6890 Å) is coincident with the expected Ly $\alpha$  emission line.

$5 \times 10^{10} M_{\odot}$  ( $4.94 < z < 5.02$ ). Turning the arguments around, i) assuming a typical  $L'_{\text{CO}} - L_{\text{FIR}}$  conversion (Riechers et al. 2006) the FIR luminosity inferred here for AzTEC 1,  $L_{\text{FIR}} = 9 \times 10^{12} L_{\odot}$ , yields an expected CO luminosity of  $L'_{\text{CO}} \approx 4 \times 10^{10} \text{ K km s}^{-1} \text{ pc}^2$ , and ii) assuming a gas-to-dust-ratio of 50–150 (e.g. Calzetti et al. 2000), and  $M_{\text{gas}}/L'_{\text{CO}} = 0.8 M_{\odot} (\text{K km s}^{-1} \text{ pc}^2)^{-1}$  the dust mass we inferred here for AzTEC 1 ( $M_{\text{D}} \sim 1.5 \times 10^9 M_{\odot}$ ) translates into a line luminosity of  $L'_{\text{CO}} \sim (9 - 30) \times 10^{10} \text{ K km s}^{-1} \text{ pc}^2$ . Such a gas reservoir should have been detected (especially with the more sensitive PdBI observations) within our interferometric observations in the 3 mm band. Below we discuss a few possibilities why the CO(5 $\rightarrow$ 4) line was not detected.

First, it is possible that the systemic redshift of the

source is outside the bandwidth range covered with our interferometric observations (encompassing redshift ranges of 4.56–4.76 and 4.94–5.02). Our UV-NIR analysis of the SED yields a 68% probability that the redshift of the source is within  $4.56 < z < 4.70$ . However, we also find a second redshift peak at  $z \sim 4.44$  in our redshift probability distribution (see Fig. 3). Furthermore, the systemic (CO) redshift of the source is not necessarily expected to coincide with the one inferred from UV-NIR data (typical velocity offsets are several hundred  $\text{km s}^{-1}$  for narrow-line objects). Thus, it is possible that the CO redshift is outside the range covered by our interferometric observations. Note however, that if this were the case, it would not significantly alter the results of our SED analysis (Sec. 4). Alternatively, assuming

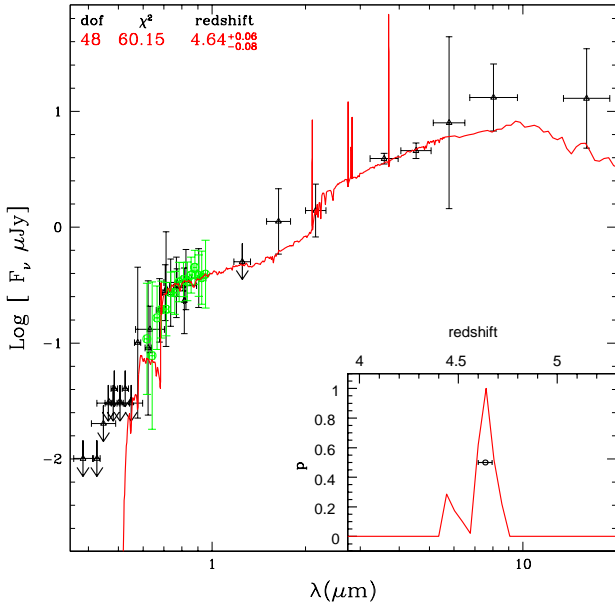


FIG. 3.— The UV-IR spectral energy distribution (SED) of AzTEC 1 (symbols). The spectral template, best fit to the multi-band photometry (filled symbols) and the binned DEIMOS spectrum (open symbols), redshifted to the most probable redshift ( $z = 4.64$ ) is also plotted (in red). The redshift probability distribution  $p \propto \exp(-0.5\chi^2)$  is shown in the inset. The median redshift and  $1\sigma$  uncertainties ( $z = 4.64^{+0.06}_{-0.08}$ ), as well as the degrees of freedom (dof) and the total  $\chi^2$  of the best fit are indicated in the top-left.

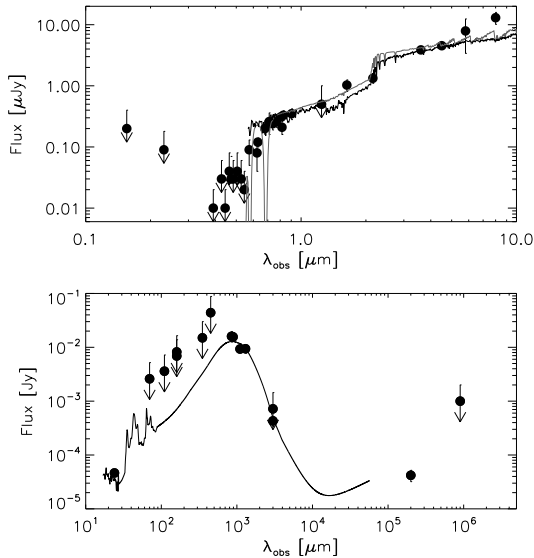


FIG. 4.— UV-NIR (top) and IR (bottom) SED of AzTEC 1. The best fit model spectra from the Maraston (2005, gray) and Bruzual et al. (2003, black) library to the UV-NIR SED and Lagache et al. (2003) library to the IR SED are also shown (see text for details).

the systemic redshift is within the covered bandwidth, the CO(5 $\rightarrow$ 4) non-detection could be explained by a low CO-excitation resulting in a low line brightness of the CO(5 $\rightarrow$ 4) transition. Assuming a CO 5 $\rightarrow$ 4 to 1 $\rightarrow$ 0 line

brightness temperature ratio of  $\sim 1/3$ , as found for the  $z > 4$  SMG GN20 (Carilli et al. 2010), the PdBI  $3\sigma$  limit in the CO(1 $\rightarrow$ 0) line is  $L'_{\text{CO}} \lesssim 3 \times 10^{10} \text{ K km s}^{-1} \text{ pc}^2$ . This is roughly consistent with the CO-FIR relation. Furthermore, an uncertainty of a factor of a few in the inferred dust mass (including possible AGN heating) and the  $M_{\text{gas}}/L'_{\text{CO}}$  conversion factor makes this limit also roughly consistent with  $L'_{\text{CO}}$  estimated from AzTEC 1's dust mass. Thus, a low CO-excitation in AzTEC 1 may explain the non-detection of CO(5 $\rightarrow$ 4).

## 5.2. Mode of star formation

Our analysis of the UV-radio SED of AzTEC 1 implies that AzTEC 1 is an extremely young and massive galaxy, forming stars at a rate of  $\sim 1300 M_{\odot} \text{ yr}^{-1}$  at  $z = 4.6$ . In general, vigorous star formation induces strong negative feedback that can terminate (and then self-regulate) the starburst by dispersing and expelling gas from the gravitational potential well (Elmegreen 1999; Scoville 2003; Thompson et al. 2005; Riechers et al. 2009). This sets a number of physical limits on the starburst. Assuming that a) the maximum intensity of a radiation-pressure supported starburst is determined by the Eddington limit for dust, b) a constant gas-to-dust ratio with radius, and c) that the disk is self-regulated (i.e. Toomre  $Q \sim 1$ ) such an Eddington limited starburst will have a SFR surface density  $\Sigma_{\text{SFR}} \sim 1000 M_{\odot} \text{ yr}^{-1} \text{ kpc}^{-2}$ , a FIR luminosity surface density  $F_{\text{FIR}} \sim 10^{13} L_{\odot} \text{ kpc}^{-2}$ , and an effective temperature of 88 K (see eqs. 33-36 in Thompson et al. 2005).

A SFR of  $\sim 1300 M_{\odot} \text{ yr}^{-1}$  in AzTEC 1 (based on the NUV-NIR SED fit) then implies a SFR surface density of  $\Sigma_{\text{SFR}} = \text{SFR}/(\pi r^2) \gtrsim 420 M_{\odot} \text{ yr}^{-1} \text{ kpc}^{-2}$  (assuming  $r \lesssim 1 \text{ kpc}$  based on SMA imaging; Younger et al. 2008). The inferred value does not violate the Eddington limited starburst models. The FIR luminosity surface density in AzTEC 1,  $F_{\text{FIR}} = L_{\text{FIR}}/(\pi r^2) \gtrsim 2.8 \times 10^{12} L_{\odot} \text{ kpc}^{-2}$ , and the dust temperature of  $\sim 50 \text{ K}$  support that the starburst in AzTEC 1 is consistent, but not in violation of its Eddington limit.

It is noteworthy that the inferred value of the SFR surface density for AzTEC 1 is somewhat higher compared to SMGs at  $z \sim 2$ , which typically have  $\Sigma_{\text{SFR}} \sim 80 M_{\odot} \text{ yr}^{-1} \text{ kpc}^{-2}$  (Tacconi et al. 2006), pointing to the compactness of the star formation region in AzTEC 1. Tacconi et al. have shown that  $z \sim 2$  SMGs are well described within a starburst picture (Elmegreen 1999) in which star formation cannot self-regulate and thus a significant fraction of gas is converted into stars in only a few times the dynamical timescale. Continuing this line of reasoning we make use of a detailed hydrodynamical study of matter deposition in young assembling galaxies performed by Silich et al. (2010). We estimate that AzTEC 1 is forming stars in a 'gravitationally bound' regime in which gravity prohibits the formation of a superwind, leading to matter accumulation within the galaxy and further generations of star formation. Specifically, Silich et al. show that there are three hydrodynamic regimes that develop in starbursting galaxies: i) generation of a superwind, that expels matter from the star forming region, ii) a 'gravitationally bound' regime, in which gravity prohibits the formation of a superwind and contains the matter within the galaxy, and iii) an

intermediate, bimodal regime. The specific regime is dependent on the SFR and the size of the star formation region in the galaxy (see Fig. 1 in Silich et al. 2010). Taking the size of the star forming region in AzTEC 1 to be  $\sim 1$  kpc (Younger et al. 2008), its SFR  $\sim 1300 M_{\odot} \text{ yr}^{-1}$  yields that, consistent with SCUBA detected galaxies, AzTEC 1 is forming stars in the gravitationally bound regime.

In summary, our analysis of the properties of AzTEC 1 points to an extremely young and massive galaxy, forming stars at a rate of  $\sim 1300 M_{\odot} \text{ yr}^{-1}$  at  $z = 4.6$ . We find that it has already assembled a stellar mass of  $1.5 \times 10^{11} M_{\odot}$ , in a region covering only  $\sim 1 - 2$  kpc in total extent (based on HST and SMA imaging; see Younger et al. 2007, 2008) yielding that AzTEC 1 is a compact massive galaxy at  $z = 4.6$ .

The high stellar mass and compactness of AzTEC 1 resemble that of a recently identified population of quiescent, passively evolving, already massive (typically  $M_{*} = 1.7 \times 10^{11} M_{\odot}$ ), but compact galaxies at  $z \sim 2$  (e.g. van Dokkum et al. 2008) deemed to evolve into the most massive red-and-dead galaxies at  $z \sim 0$ . The upper gas mass limit inferred for AzTEC 1 (although quite uncertain) is  $\sim 10^{10} M_{\odot}$ . If AzTEC 1 continues to form stars at the current rate it will deplete the available gas in  $M_{\text{gas}}/\text{SFR} \sim 6$  Myr (assuming 100% efficiency). Unless further gas is supplied and high levels of star formation are induced the galaxy's stellar body will have time to age and redden till  $z \sim 2 - 3$ .

The surface density of the (likely still incomplete) sample of three confirmed  $z > 4$  SMGs in the AzTEC-COSMOS field ( $0.3 \text{ deg}^2$ ) is  $\gtrsim 10 \text{ deg}^{-2}$ . This is already higher than  $\sim 7 \text{ deg}^{-2}$  predicted by semi-analytic models of structure growth (e.g. Baugh et al. 2005; see also Coppin et al. 2009, 2010). Thus, further studies of  $z > 4$  SMGs are key to understand the SMG population (e.g. Wall et al. 2008) and its cosmological role.

## 6. CONCLUSIONS

Based on UV-FIR observations of AzTEC 1, and a Keck II/DEIMOS spectrum, we have shown that AzTEC 1 is a  $L_{\text{FIR}} = 9 \times 10^{12} L_{\odot}$  starburst at  $z = 4.64_{-0.08}^{+0.06}$  (with a secondary, less likely, redshift probability peak at  $z \sim 4.44$ ). Based on our revised FIR values we find that AzTEC 1 fits comfortably within the limits of a maximal starburst, and that it forms stars in a gravitationally bound regime which traps the gas within the galaxy leading to formation of new generations of stars. Our SED analysis yields that AzTEC 1 is an extremely young ( $\lesssim 50$  Myr), massive ( $M_{*} \sim 10^{11} M_{\odot}$ ), but compact ( $\lesssim 2$  kpc) galaxy forming stars at a rate of  $\sim 1300 M_{\odot} \text{ yr}^{-1}$  at  $z = 4.64$ . These interesting properties suggest that AzTEC 1 may be a candidate of progenitors of quiescent, already massive, but very compact galaxies regularly found at  $z \sim 2$ , and thought to evolve into the most massive, red-and-dead galaxies found in the local universe.

The authors acknowledge the significant cultural role that the summit of Mauna Kea has within the indigenous Hawaiian community; NASA grants HST-GO-09822 (contracts 1407, 1278386; SSC); HST-HF-51235.01 (contract NAS 5-26555; STScI); GO7-8136A; Blancheflor Boncompagni Ludovisi foundation (F.C.); French Agence National de la Recherche fund ANR-07-BLAN-0228; CNES; Programme National Cosmologie et Galaxies; UKF; DFG; DFG Leibniz Prize (FKZ HA 1850/28-1); European Union's Seventh Framework programme (grant agreement 229517); making use of the NASA/ IPAC IRSA, by JPL/Caltech, under contract with the National Aeronautics and Space Administration; IRAM PdBI supported by INSU/CNRS (France), MPG (Germany) and IGN (Spain); CARMA supported by the states of California, Illinois, and Maryland, the Gordon and Betty Moore Foundation, the Eileen and Kenneth Norris Foundation, the Caltech Associates, and NSF.

## REFERENCES

- Aravena, M., et al. 2008, *A&A*, 491, 173  
Aretxaga, I., Hughes, D. H., Chapin, E. L., Gaztañaga, E., Dunlop, J. S., & Ivison, R. J. 2003, *MNRAS*, 342, 759  
Baugh, C. M., Lacey, C. G., Frenk, C. S., Granato, G. L., Silva, L., Bressan, A., Benson, A. J., & Cole, S. 2005, *MNRAS*, 356, 1191  
Berta, S., et al. 2010, *A&A*, 518, L30  
Blain, A. W., Smail, I., Ivison, R. J., Kneib, J.-P., & Frayer, D. T. 2002, *Phys. Rep.*, 369, 111  
Bruzual G., Charlot S., 2003, *MNRAS*, 344, 1000  
Capak, P., et al. 2007, *ApJS*, 172, 99  
Capak, P., et al. 2008, *ApJ*, 681, L53  
Capak, P., et al. 2010, *Nature*, accepted  
Carilli, C. L., et al. 2010, *ApJ*, 714, 1407  
Cimatti, A., et al. 2008, *A&A*, 482, 21  
Chapman, S. C., Blain, A. W., Smail, I., & Ivison, R. J. 2005, *ApJ*, 622, 772  
Chary, R., & Elbaz, D. 2001, *ApJ*, 556, 562  
Coppin, K. E. K., et al. 2009, *MNRAS*, 395, 1905  
Coppin, K. E. K., et al. 2010, *MNRAS*, 407, L103  
Daddi, E., et al. 2009a, *ApJ*, 694, 1517  
Daddi, E., Dannerbauer, H., Krips, M., Walter, F., Dickinson, M., Elbaz, D., & Morrison, G. E. 2009b, *ApJ*, 695, L176  
Dale, D. A., & Helou, G. 2002, *ApJ*, 576, 159  
Elmegreen, B. G. 1999, *ApJ*, 517, 103  
Elvis, M., et al. 2009, *ApJS*, 184, 158  
Efstathiou, A., Rowan-Robinson, M., & Siebenmorgen, R. 2000, *MNRAS*, 313, 734  
Faber, S. M., et al. 2007, *ApJ*, 665, 265  
Ilbert, O., et al. 2009, *ApJ*, 690, 1236  
Kennicutt, R. C., Jr. 1998, *ARA&A*, 36, 189  
Knudsen, K. K., Kneib, J.-P., Richard, J., Petitpas, G., & Egami, E. 2010, *ApJ*, 709, 21  
Koekemoer, A. M. et al. 2007, *ApJS* 172, 196  
Lagache, G., Dole, H., & Puget, J.-L. 2003, *MNRAS*, 338, 555  
Leauthaud, A., et al. 2007, *ApJS*, 172, 219  
Maraston, C. 2005, *MNRAS*, 362, 799  
Maraston, C., Pforr, J., Renzini, A., Daddi, E., Dickinson, M., Cimatti, A., & Tonini, C. 2010, *MNRAS*, 407, 830  
Riechers, D. A., et al. 2006, *ApJ*, 650, 604  
Riechers, D. A., et al. 2009, *ApJ*, 703, 1338  
Riechers, D. A., et al. 2010, *ApJ*, 720, L131  
Sanders, D. B., et al. 2007, *ApJS*, 172, 86  
Schinnerer, E., et al. 2007, *ApJS*, 172, 46  
Schinnerer, E., et al. 2008, *ApJ*, 689, L5  
Schinnerer, E., et al. 2010, *ApJS*, 188, 384  
Shapley, A. E., Steidel, C. C., Pettini, M., & Adelberger, K. L. 2003, *ApJ*, 588, 65  
Silich, S., Tenorio-Tagle, G., Muñoz-Tuñón, C., Hueyotl-Zahuantitla, F., Wünsch, R., & Palouš, J. 2010, *ApJ*, 711, 25  
Scott, K. S., et al. 2008, *MNRAS*, 385, 2225

TABLE 1  
AzTEC 1 PHOTOMETRY

wavelength	band/telescope	flux density ( $\mu\text{Jy}$ )
0.5-2 keV	Chandra-soft-band	$< 0.0003^{a,b}$
1551Å	FUV	$< 0.20^a$
2307Å	NUV	$< 0.09^a$
3911Å	u*	$< 0.01^a$
4270Å	IA427	$< 0.03^a$
4440Å	B <sub>J</sub>	$< 0.01^a$
4640Å	IA464	$< 0.04^a$
4728Å	g <sup>+</sup>	$< 0.03^a$
4840Å	IA484	$< 0.03^a$
5050Å	IA505	$< 0.04^a$
5270Å	IA527	$< 0.03^a$
5449Å	V <sub>J</sub>	$< 0.02^a$
5740Å	IA574	$0.09 \pm 0.04$
6240Å	IA624	$0.08 \pm 0.04$
6295Å	r <sup>+</sup>	$0.12 \pm 0.02$
6790Å	IA679	$0.20 \pm 0.04$
7090Å	IA709	$0.25 \pm 0.04$
7110Å	NB711	$0.26 \pm 0.10$
7380Å	IA738	$0.24 \pm 0.05$
7641Å	i <sup>+</sup>	$0.29 \pm 0.02$
7670Å	IA767	$0.26 \pm 0.05$
8040Å	F814W	$0.31 \pm 0.02$
8150Å	NB816	$0.21 \pm 0.05$
8270Å	IA827	$0.33 \pm 0.06$
9037Å	z <sup>+</sup>	$0.35 \pm 0.07$
12444Å	J	$< 0.5^a$
16310Å	H	$1.03 \pm 0.22$
21537Å	K <sub>s</sub>	$1.33 \pm 0.23$
3.6 $\mu\text{m}$	IRAC1	$3.87 \pm 0.13$
4.5 $\mu\text{m}$	IRAC2	$4.53 \pm 0.23$
5.8 $\mu\text{m}$	IRAC3	$7.90 \pm 4.50$
8.0 $\mu\text{m}$	IRAC4	$13.01 \pm 2.88$
16 $\mu\text{m}$	IRS-16	$12.80 \pm 4.20$
24 $\mu\text{m}$	MIPS-24	$46.40 \pm 4.90$
70 $\mu\text{m}$	MIPS-70	$< 2600^a$
100 $\mu\text{m}$	PACS-100	$< 3600^a$
160 $\mu\text{m}$	MIPS-160	$< 8200^a$
160 $\mu\text{m}$	PACS-160	$< 6900^a$
350 $\mu\text{m}$	CSO	$< 15000^a$
450 $\mu\text{m}$	SCUBA-2	$< 44000^a$
850 $\mu\text{m}$	SCUBA-2	$16000 \pm 3500$
890 $\mu\text{m}$	SMA	$15600 \pm 1100$
1.1 mm	JCMT/AzTEC	$9300 \pm 1300$
1.3 mm	CARMA	$9400 \pm 1600$
3 mm	CARMA	$< 720^a$
3 mm	PdBI	$300 \pm 40$
20 cm	VLA	$42.0 \pm 10$
90 cm	VLA	$< 1000^a$

<sup>a</sup> The given limits are  $2\sigma$  upper limits. <sup>b</sup> Corresponds to  $= 10^{-15}$  erg cm<sup>-2</sup> s<sup>-1</sup>

Scoville, N., et al. 2007, ApJS, 172, 1

Smolčić, V., et al. 2008, ApJS, 177, 14

Tacconi, L. J., et al. 2006, ApJ, 640, 228

Thompson, T. A., Quataert, E., & Murray, N. 2005, ApJ, 630, 167

van Dokkum, P. G., et al. 2008, ApJ, 677, L5

Wall, J. V., Pope, A., & Scott, D. 2008, MNRAS, 383, 435

Younger, J. D., et al. 2007, ApJ, 671, 1531

Younger, J. D., et al. 2008, ApJ, 688, 59

Yun, M. S., & Carilli, C. L. 2002, ApJ, 568, 88

Zamojski, M. A., et al. 2007, ApJS, 172, 468